SPARSE-VIEW X-RAY SPECTRAL CT RECONSTRUCTION USING ANNIHILATING FILTER-BASED LOW RANK HANKEL MATRIX APPROACH

Yo Seob Han[1], *Kyong Hwan Jin*[1], *Kyungsang Kim*[2], *Jong Chul Ye*[1]

[1]Bio-Imaging and Signal Processing Lab. (BISPL), Dept. Bio & Brain Engineering
Korea Advanced Institute of Science & Technology (KAIST)
[2]Center for Advanced Medical Imaging Sciences
Massachusetts General Hospital and Harvard Medical School

ABSTRACT

In a kVp switching-based sparse view spectral CT, each spectral image cannot be reconstructed separably by an analytic reconstruction method, because the projection views for each spectral band is too sparse. However, the underlying structure is common between the spectral bands, so there exists inter-spectral redundancies that can be exploited by the recently proposed annihilating filter-based low rank Hankel matrix approach (ALOHA). More specifically, the sparse view projection data are first rebinned in the Fourier space, from which Hankel structured matrix with missing elements are constructed for each spectral band. Thanks to the inter-spectral correlations as well as transform domain sparsity of underlying images, the concatenated Hankel structured matrix is low-ranked, and the missing Fourier data for each spectral band can be simultaneously estimated using a low rank matrix completion. To reduce the computational complexity furthermore, we exploit the Hermitian symmetry of Fourier data. Numerical experiments confirm that the proposed method outperforms the existing ones.

Index Terms— spectral computed tomography (CT), sparse-view X-ray CT, annihilating filter, low rank Hankel matrix

1. INTRODUCTION

X-ray computed tomography (CT) has been widely used for diagnosis. Recently, for various applications such as tissue characterization and material decomposition, spectral CT has been developed. Note that the tissue or material components can be distinguished via multiple X-ray energy spectra, because the attenuation coefficients of the components varies along the spectral energy. However, compared to the single spectral CT, the total radiation dose increases in proportion to the number of spectral bins. To reduce the radiation dose, a sparse-view spectral CT was investigated [1]. More specifically, as illustrated in Fig 1(a), in this method, the X-ray sources are switched sequentially. However, the projection view for each spectrum is sparse, so it is difficult to use an analytic reconstruction.

To address this issue, total variation (TV) regularization [2] term could be used. However, due to the simple spatial domain constraint that does not exploit the spectral domain correlation, the reconstruction quality improvement is limited. To exploit the spectral redundancies, several methods have been proposed, among which robust PCA approach is well-known [3]. Specially, the algorithm PRISM (prior rank, intensity, and sparsity model) [3] estimates low-rank and sparse components by modeling the common spectral image domain feature as a low rank component.

In this paper, we propose a drastically different approach for sparse-view spectral CT. Rather than exploiting the spectral redundancy as a penalty function, the method is based on a novel Fourier domain interpolation method that exploits both spectral redundancies as well as transform domain sparsity of the underlying images. Then, the final reconstruction images for each spectral band can be obtained using simple FFT algorithms. In fact, one of the most important contributions is that the spectral redundancies as well as transform domain sparsity can be exploited by using recently proposed annihilating filter-based low rank Hankel matrix (ALOHA) approaches [4, 5]. By utilizing this property, the Fourier domain interpolation can be performed as a low rank Hankel structured matrix completion problem. Numerical reconstruction results clearly showed that the proposed algorithm outperforms the existing ones.

2. THEORY

2.1. Annihilation Property in Spectral CT

Let $x_i(\mathbf{r})$ denotes the i-th spectrum images. In our spectral CT model, we assume that the spectral image can be represented as

$$x_i(\mathbf{r}) = s_i(\mathbf{r})f(\mathbf{r}),$$

where $f(\mathbf{r})$ is the underlying common structure image and $s_i(\mathbf{r})$ is the spectral sensitivity. We further assume that the spectral sensitivity is sufficiently smooth. Then, under the assumption that the underlying structure can be represented as

This work is supported by the grant from Korean Government (NRF-2014R1A2A1A11052491).

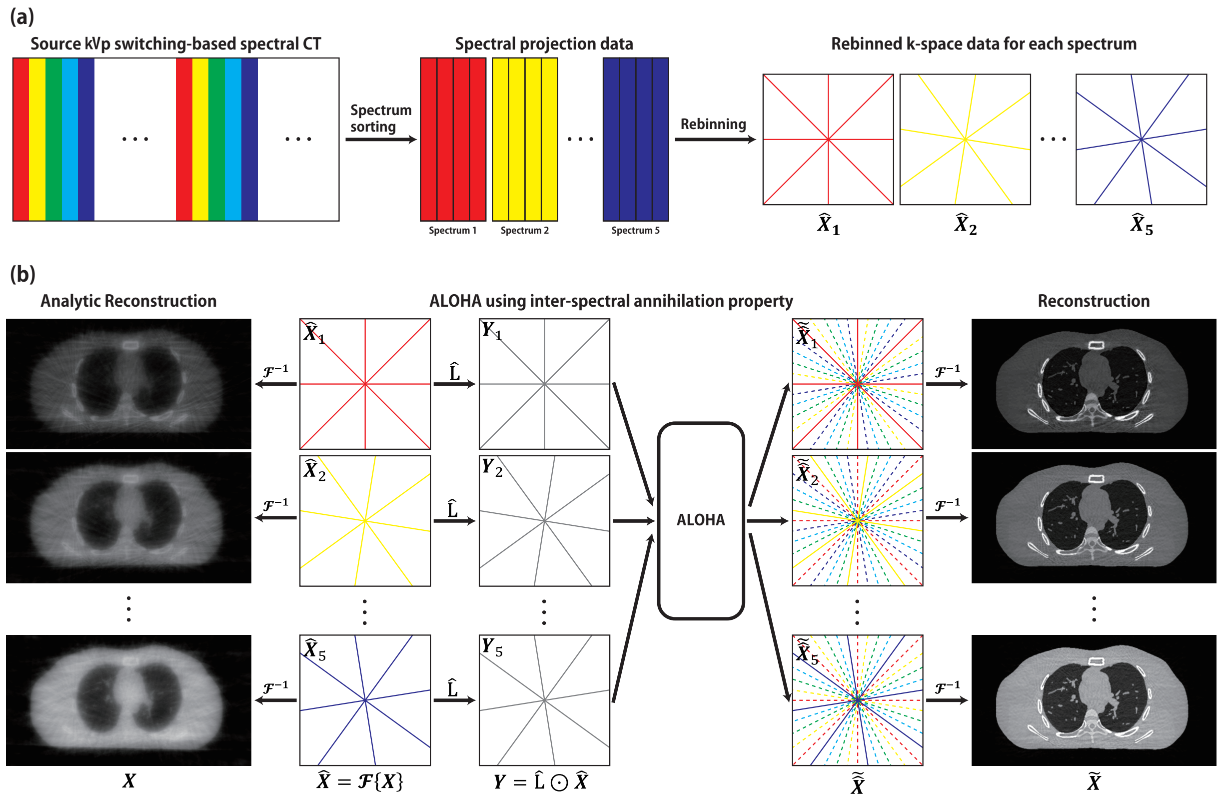

Fig. 1. (a) For each spectral band projection data, the corresponding Fourier data with missing elements are obtained by rebinning the data. (b) Spectral CT reconstruction framework. After missing views are interpolated in Fourier domain by utilizing the inter-spectral redundancies and the transform domain sparsity, each spectral image is obtained using a simple FFT.

the sum of spline surfaces, we have the following approximation:

$$\begin{aligned} Lx_i(\mathbf{r}) &\simeq s_i(\mathbf{r})Lf(\mathbf{r}) \\ &= s_i(\mathbf{r})\sum_{k=1}^{K} c_k\delta(\mathbf{r}-\mathbf{r}_k) \\ &\simeq \sum_{k=1}^{K} c_k s_i(\mathbf{r}_k)\delta(\mathbf{r}-\mathbf{r}_k), \end{aligned} \tag{1}$$

where L denotes the sparsifying transform operator such as differential operator (which will be explained later furthermore), and $\{\mathbf{r}_k\}$ denotes the discontinuity locations. For the case of 2D images, the singularity is represented as curves, and the aforementioned Dirac model may not be accurate, but still serves our goal in discrete implementation. For exact representation of 2D signals, see [6]. Then, the corresponding Fourier transform is given by

$$\begin{aligned} \boldsymbol{\mathcal{F}}\{Lx_i(\mathbf{r})\} &= \hat{l}(\boldsymbol{\omega})\hat{x}_i(\boldsymbol{\omega}) \\ &= \sum_{k=1}^{K} c_k s_i(\mathbf{r}_k)e^{-j2\pi\mathbf{k}^T\mathbf{r}_k}, \end{aligned} \tag{2}$$

where $\hat{l}(\boldsymbol{\omega})$ denotes the spectrum of the sparsifying transform. Since the right hand side term is given as the sum of harmonics, there exists annihilating filter $\hat{h}_i(\boldsymbol{\omega})$ such that

$$\hat{h}_i(\boldsymbol{\omega}) * \hat{l}(\boldsymbol{\omega})\hat{x}_i(\boldsymbol{\omega}) = 0. \tag{3}$$

In addition, we can exploit the annihilation property from the inter-spectral annihilating relationship given as

$$\hat{s}_j(\boldsymbol{\omega}) * \left(\hat{l}(\boldsymbol{\omega})\hat{x}_i(\boldsymbol{\omega})\right) - \hat{s}_i(\boldsymbol{\omega}) * \left(\hat{l}(\boldsymbol{\omega})\hat{x}_j(\boldsymbol{\omega})\right) = 0, \quad \forall\boldsymbol{\omega}, \quad i \neq j. \tag{4}$$

Accordingly, we construct a concatenated 2D Hankel matrix

$$\boldsymbol{\mathcal{X}} = \begin{bmatrix} \mathscr{H}\{\widehat{\mathbf{L}}\odot\widehat{\mathbf{X}}_1\} & \cdots & \mathscr{H}\{\widehat{\mathbf{L}}\odot\widehat{\mathbf{X}}_E\} \end{bmatrix}, \tag{5}$$

where $\widehat{\mathbf{L}}$ denotes the weighting matrix constructed from discrete samples of $\hat{l}(\boldsymbol{\omega})$, $\widehat{\mathbf{X}}_i$ denotes the discrete samples of $\hat{x}_i(\boldsymbol{\omega})$, $\odot$ denotes the Hadamard product and $\mathscr{H}\{\widehat{F}\}$ is represented as

$$\mathscr{H}\{\widehat{F}\} = \begin{bmatrix} \mathcal{H}\{\hat{\mathbf{f}}_0\} & \mathcal{H}\{\hat{\mathbf{f}}_1\} & \cdots & \mathcal{H}\{\hat{\mathbf{f}}_{q-1}\} \\ \mathcal{H}\{\hat{\mathbf{f}}_1\} & \mathcal{H}\{\hat{\mathbf{f}}_2\} & \cdots & \mathcal{H}\{\hat{\mathbf{f}}_q\} \\ \vdots & \vdots & \ddots & \vdots \\ \mathcal{H}\{\hat{\mathbf{f}}_{n-q}\} & \mathcal{H}\{\hat{\mathbf{f}}_{n-q+1}\} & \cdots & \mathcal{H}\{\hat{\mathbf{f}}_{m-1}\} \end{bmatrix},$$

with $\mathcal{H}\{\hat{\mathbf{f}}_j\} \in \mathbb{C}^{(m-p+1)\times p}$ denotes the 1D Hankel matrix for the j-th column of $\widehat{F}$, $m \times n$ and $p \times q$ denote the size of image and filter, respectively. Then, it is easy to show that

$$\boldsymbol{\mathcal{X}}\mathcal{S}_1 = \mathbf{0},$$

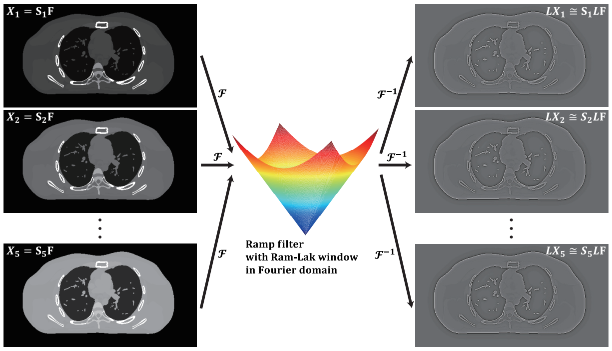

Fig. 2. Sparse transform using a ramp filter with Ram-Lak window.

where $\mathcal{S}_1$ is defined recursively as follows:

$$\mathcal{S}_{E-1} \triangleq \begin{bmatrix} \bar{\mathbf{s}}_E \\ -\bar{\mathbf{s}}_{E-1} \end{bmatrix} \tag{6}$$

$$\mathcal{S}_t \triangleq \left[\begin{array}{cccc|c} \bar{\mathbf{s}}_{t+1} & \bar{\mathbf{s}}_{t+2} & \cdots & \bar{\mathbf{s}}_E & \mathbf{0} \\ \hline -\bar{\mathbf{s}}_t & & & & \\ & -\bar{\mathbf{s}}_t & & & \mathcal{S}_{t+1} \\ & & \ddots & & \\ & & & -\bar{\mathbf{s}}_t & \end{array}\right], \tag{7}$$

and $\bar{\mathbf{s}}_i := \overline{\textsc{vec}(\hat{s}_i)}$ denotes the reversed ordered, vectored spectral modulation filter for the i-th channel. Because $\dim \textsc{Nul}(\boldsymbol{\mathcal{X}}) = \operatorname{rank}(\mathcal{S}_1) = \binom{E}{2} = E(E-1)/2$, we have

$$\operatorname{rank} \boldsymbol{\mathcal{X}} \leq kE - \frac{E(E-1)}{2} = \frac{E(2k-E+1)}{2}. \tag{8}$$

Therefore, $\boldsymbol{\mathcal{X}}$ matrix is low-ranked, and the missing element can be recovered by solving the following low rank matrix completion problem:

$$\begin{aligned} \min_{\boldsymbol{\mathcal{X}}} \quad & \|\boldsymbol{\mathcal{X}}\|_* \\ \text{subject to} \quad & \boldsymbol{\mathcal{X}} = \left[\mathscr{H}\{\widehat{\mathbf{M}}_1\} \quad \cdots \quad \mathscr{H}\{\widehat{\mathbf{M}}_E\}\right] \\ & P_\Omega(\widehat{\mathbf{M}}_i) = P_\Omega(\widehat{\mathbf{L}} \odot \widehat{\mathbf{X}}_i), \quad i = 1, \cdots, E, \end{aligned} \tag{9}$$

and Ω denotes the sampling indices and P_Ω is the projection operator on the index set Ω. This optimization problem can be solved using a SVD-free structured matrix minimization using ADMM [4, 5]. Specifically, the associate Lagrangian cost function is given by

$$\begin{aligned} L(\mathbf{U}, \mathbf{V}, \boldsymbol{\mathcal{X}}, \boldsymbol{\Lambda}) := \quad & \iota_\Omega(\boldsymbol{\mathcal{X}}) + \tfrac{1}{2}\left(\|\mathbf{U}\|_F^2 + \|\mathbf{V}\|_F^2\right) \\ & + \tfrac{\mu}{2}\|\boldsymbol{\mathcal{X}} - \mathbf{U}\mathbf{V}^H + \boldsymbol{\Lambda}\|_F^2, \end{aligned} \tag{10}$$

where $\iota_\Omega(\boldsymbol{\mathcal{X}})$ denotes the indicator function. To minimize the cost function $L(\mathbf{U}, \mathbf{V}, \boldsymbol{\mathcal{X}}, \boldsymbol{\Lambda})$, we employed a Alternating Direction Method of Multipliers (ADMM) [4, 5].

2.2. Choice of Sparse Transform

Among the various choices of sparsifying transforms, here we chose the ramp filtering with Ram-Lak window. The motivation for this choice is that this weighting is widely used as a filtering process for filtered back projection (FBP) algorithms in CT, and it produces edge images as shown in Fig 2 if we directly apply FFT type inversion without density compensation. Moreover, unlike the Laplacian weighting or TV weighting, the ramp filter with Ram-Lak weighting can control the noise boosting, which improves the performance of low rank matrix completion in ALOHA.

In fact, one of the powerful nature of ALOHA is that even though a sparsity imposing transform is not explicitly represented in spatial domain, as long as the corresponding spatial image can be sparsified using a corresponding Fourier weighting, the associated Hankel matrix in k-space is low-ranked, which can be exploited to estimate the missing k-space data.

2.3. Complexity Reduction by Symmetry

In a kVp switching-based spectral CT, each spectral data is sparsely sampled along the angle. Accordingly, the annihilating filter size for ALOHA should be bigger than the maximum gap of radial sample. However, if the filter size is too big, then the computation complexity increases significantly. To reduce the computational complexity, we exploit the symmetry of spectral data. Specifically, in spectral CT, the images should be real-valued, so its k-space data should satisfy the Hermitian symmetry. Thanks to the symmetry, the proposed method is applied to the half of k-space, after which the remaining part of k-space data is easily estimated. Moreover, we can apply the proposed method to each quadrant separately.

3. RESULTS

Our switching-based spectral CT system was simulated using a parallel-beam geometry, but can be easily extended to fan-beam geometry. For numerical experiments, we used 2D XCAT phantoms which have difference linear attenuation coefficients on five spectral bands such as 30, 45, 60, 75, and 90 kVp. The phantom is 512×512 pixels, and the detector array is 729 elements. For each spectral projection data, the number of views was 24 views, so total 120 views were acquired for all spectral projection data. The performance of the proposed method was compared with those of the reconstruction results by TV [2], and RPCA [3]. To evaluate the performance quantitatively, the normalized mean square error (NMSE) value were calculated.

Fig 3 shows the ground truth, and the reconstruction results by TV, RPCA, and the proposed method. The TV method does not consider the relationship between the spectral images, which resulted in the severe distortion. The RPCA method improved the structural component better than the TV, since the RPCA method uses the spectral correlation. However, there were significant blurring. Compared to the other reconstruction results, the proposed method did not

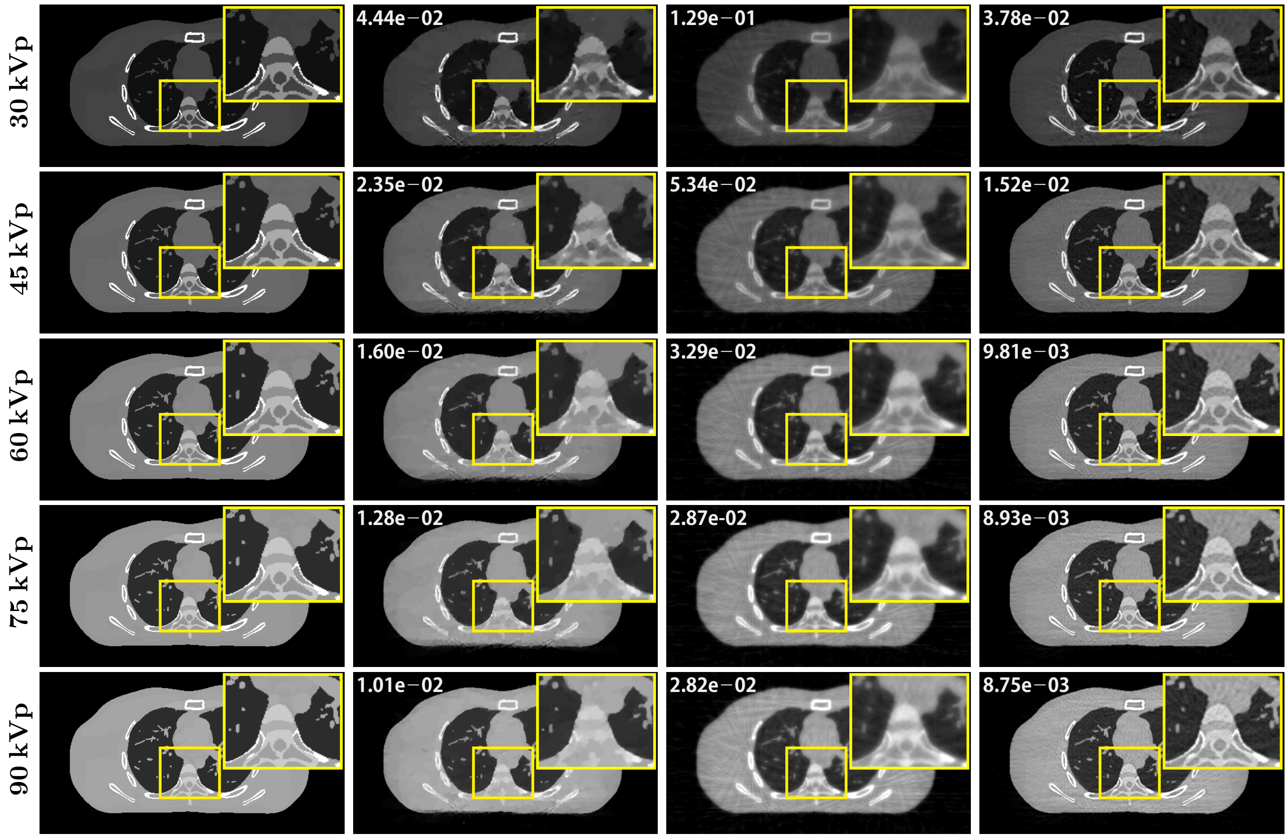

(a) **Phantom** (b) **TV** (c) **RPCA** (d) **Proposed**

Fig. 3. The first column is ground truth for each spectrum. From the second to last column, each column illustrates reconstructed images by TV for single-spectral sparse view, RPCA, and proposed method, respectively. Each row represents spectral images at 30 kVp, 45 kVp, 60 kVp, 75 kVp, and 90 kVp. The NRMS value is written at the corner of the results.

produce any structural distortion and blurring effect. Furthermore, NMSE value is lower than other reconstruction results.

4. CONCLUSION

We proposed a novel reconstruction algorithm for a kVp switching-based sparse-view spectral CT problem using the recently proposed ALOHA algorithm. Even though each spectral data is too sparse to provide high quality reconstruction, by exploiting annihilation property originated from inter-spectral redundancy and transform domain sparsity, the missing Fourier data can be interpolated by a low rank Hankel matrix completion algorithm. Additionally, to reduce the computation complexity of the proposed method, we exploited the Hermitian symmetry of the Fourier data. Reconstruction results clearly demonstrated that the proposed method outperforms the existing spectral CT algorithms.

5. REFERENCES

[1] Kyungsang Kim, Jong Chul Ye, William Worstell, Jinsong Ouyang, Yothin Rakvongthai, Georges El Fakhri, and Quanzheng Li, "Sparse-view spectral CT reconstruction using spectral patch-based low-rank penalty," *IEEE Transactions on Medical Imaging*, vol. 34, no. 3, pp. 748–760, 2015.

[2] Tom Goldstein and Stanley Osher, "The split Bregman method for l_1-regularized problems," *SIAM Journal on Imaging Sciences*, vol. 2, no. 2, pp. 323–343, 2009.

[3] Stanley Osher Hao Gao, Hengyong Yu and Ge Wang, "Multi-energy CT based on a prior rank, intensity and sparsity model (PRISM)," in *2014 IEEE Global Conference on Signal and Information Processing (GlobalSIP)*. IEEE, 2014, pp. 483–486.

[4] Kyong Hwan Jin, Dongwook Lee, and Jong Chul Ye, "A general framework for compressed sensing and parallel MRI using annihilating filter based low-rank Hankel matrix," *arXiv preprint arXiv:1504.00532*, 2015.

[5] Kyong Hwan Jin and Jong Chul Ye, "Annihilating filter based low rank Hankel matrix approach for image inpainting," *IEEE Transactions on Image Processing*, vol. 24, no. 11, pp. 3498–3511, 2015.

[6] Greg Ongie and Mathews Jacob, "Off-the-grid recovery of piecewise constant images from few Fourier samples," *arXiv preprint arXiv:1510.00384*, 2015.